

High-Throughput Study of the Cu(CH₃COO)₂·H₂O–5-Nitroisophthalic Acid–Heterocyclic Ligand System: Synthesis, Structure, Magnetic, and Heterogeneous Catalytic Studies of Three Copper Nitroisophthalates

Debajit Sarma,[†] K. V. Ramanujachary,[‡] Norbert Stock,[§] and Srinivasan Natarajan*,[†]

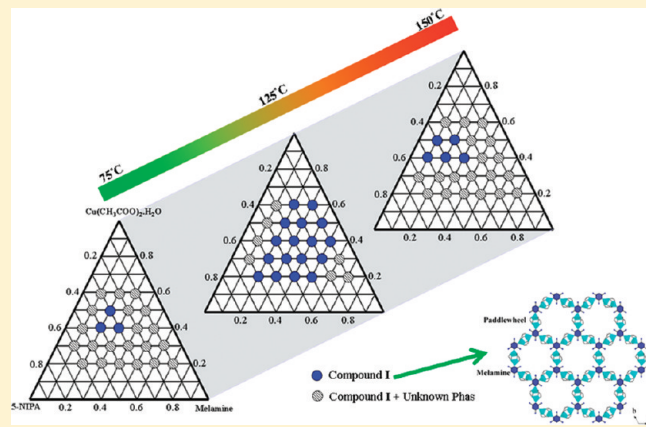
[†]Framework Solids Laboratory, Solid State and Structural Chemistry Unit, Indian Institute of Science, Bangalore-560012, India

[‡]Department of Chemistry and Biochemistry, Rowan University, 201 Mullica Hill Road, Glassboro, New Jersey, 08028, United States

[§]Institute of Inorganic Chemistry, Christian Albrechts University, Otto-Hahn-Platz 6/7, D 24118, Kiel, Germany

Supporting Information

ABSTRACT: A high-throughput screening was employed to identify new compounds in Cu(CH₃COO)₂·H₂O–NIPA–heterocyclic ligand systems. Of the compounds identified, three compounds, [Cu₃{(NO₂)–C₆H₃–(COO)₂}₃(C₃N₆H₆)] (**I**), [Cu₂(μ₃-OH)(H₂O){(NO₂)–C₆H₃–(COO)₂}({CN₄H})]·(H₂O) (**II**), and [Cu₂(μ₃-OH)(H₂O){(NO₂)–C₆H₃–(COO)₂}·(CN₅H₂)]·2(H₂O) (**III**), have been isolated as good quality single crystals by employing conventional hydrothermal methods. Three other compounds, Cu₂{(NO₂)–C₆H₃–(COO)₂}·(CN₄H)(H₂O) (**IIa**), Cu₂{(NO₂)–C₆H₃–(COO)₂}·(CN₅H₂) (**IIIa**), and Cu₂{(NO₂)–C₆H₃–(COO)₂}·{(CN₅H₂)₂}·2H₂O (**IIIb**), were identified by a combination of elemental analysis, thermogravimetric analysis (TGA), and IR spectroscopic studies, although their structures are yet to be determined. The single crystalline compounds were also characterized by elemental analysis, TGA, IR, UV-vis, magnetic, and catalytic studies. The structures of the compounds have paddle wheel (**I**) and infinite Cu–O(H)–Cu chains (**II** and **III**) connected with NIPA and heterocyclic ligands forming two- (**II**) and three-dimensional (**I** and **III**) structures. The bound and lattice water molecules in **II** and **III** could be reversibly removed/inserted without affecting the structure. In the case of **II**, the removal of water gives rise to a structural transition, but the dehydrated phase reverts back to the original phase on prolonged exposure to atmospheric conditions. Magnetic studies indicate an overall antiferromagnetism in all of the compounds. Lewis acid catalytic studies indicate that compounds **II** and **III** are active for cyanosilylation of imines.



INTRODUCTION

The design and synthesis of inorganic coordination polymers or metal organic frameworks (MOFs) continue to be of interest for their potential as well as actual use in gas storage, separation, and catalysis.¹ MOFs provide unique opportunities to control the formation of new structures by fine-tuning the organic and the inorganic component.² In addition, the well-established principles of supramolecular assembly can be employed fruitfully in the preparation of important targeted MOF structures.³ The control achieved in the design and the synthesis of MOFs creates opportunities to investigate wide-ranging properties, which are being pursued vigorously. One of the interest in transition metal-based MOFs is to study and correlate the structure with the magnetic behavior.⁴ Long-range magnetic interactions and ordering can be achieved through significant orbital overlap between the participating transition metal center and the ligands. Strong magnetic interactions are generally associated with

compounds having metal clusters or extended –M–O–M–linkages.⁵

Of the many MOFs that have been prepared and characterized, those belonging to terephthalic acid (1,4-BDC) and trimesic acid (1,3,5-BTC) appear to be the dominant ones. The combination of 1,4-BDC and transition elements has given rise to many new compounds, which exhibit interesting magnetic behavior.⁶ Similarly, the 1,3,5-BTC has also given rise to important compounds, most notably the copper compound, [Cu₃(1,3,5-BTC)₂(H₂O)₃]_n (HKUST-1).⁷ The angular disposition between the three carboxylic acid groups in the trimesic acid (120°) along with the rigid aromatic backbone has been exploited by many research groups, to form new compounds, establishing the versatility of trimesic acid as a good linker.⁸ Some

Received: November 30, 2010

Revised: January 29, 2011

Published: March 07, 2011

of the metal–trimesate compounds also exhibit interesting magnetic properties.⁹

Substitution of one of the carboxylic acid groups in trimesic acid not only would break the symmetry but also give rise to differences in its binding with suitable metal centers. One such organic linker would be 5-nitroisophthalic acid. The nitro group of the 5-nitroisophthalic acid, on the other hand, could provide useful variations by performing the role of (i) a possible hydrogen bond acceptor, (ii) an electron-donating group, and (iii) improving the reactivity. In spite of the advantages offered by the 5-nitroisophthalic acid, the usefulness of the acid as a possible linker in the assembly of MOFs has not been exploited in detail.¹⁰

In synthesizing MOFs, there have been many different approaches, which are broadly based on the trial and error methodology. Recent research has established that the high-throughput (HT) approach is very versatile and paves the way for the systematic screening of a multicomponent system.¹¹ Yaghi and co-workers have exploited this method for the identification and study of a family of ZIFs (zeolitic imidazolate frameworks).¹²

We have been interested in exploring the reactivity of 5-nitroisophthalic acid with copper salts. To this end, we have employed the HT approach. Our efforts have resulted in the identification of three distinct phases: $[\text{Cu}_3\{\text{(NO}_2\}-\text{C}_6\text{H}_3-\text{(COO})_2\}_3(\text{C}_3\text{N}_4\text{H}_6)]$ (**I**), $[\text{Cu}_2(\mu_3\text{-OH})(\text{H}_2\text{O})\{\text{(NO}_2\}-\text{C}_6\text{H}_3-\text{(COO})_2\}(\text{CN}_4\text{H})]\cdot(\text{H}_2\text{O})$ (**II**), and $[\text{Cu}_2(\mu_3\text{-OH})(\text{H}_2\text{O})\{\text{(NO}_2\}-\text{C}_6\text{H}_3-\text{(COO})_2\}(\text{CN}_5\text{H}_2)]\cdot2(\text{H}_2\text{O})$ (**III**). Here, we describe the synthesis, structure, magnetic, and preliminary studies on heterogeneous catalytic properties of the three copper nitroisophthalate compounds.

■ EXPERIMENTAL SECTION

Synthesis and Initial Characterization. The initial HT screening was carried out in a reactor block with 24 cavities containing Teflon liners (4 × 6 array). The volume of the individual Teflon reactors was 2 mL, and the reactor block was sealed inside a stainless steel autoclave. For the HT reactions, the reagent concentrations were as follows: $\text{Cu}(\text{CH}_3\text{COO})_2\cdot\text{H}_2\text{O}$, 0.02–0.06 mmol; 5-nitroisophthalate (NIPA), 0.01–0.06 mmol; and heterocyclic ligand, 0.01–0.08 mmol. Typically, prepared were the following solutions: 0.2 M solution of $\text{Cu}(\text{CH}_3\text{COO})_2\cdot\text{H}_2\text{O}$ in water and 0.2 M solution of NIPA, melamine, and aminotetrazole in methanol. The terazole was used as received (30% in acetonitrile). In a model reaction mixture, $\text{Cu}(\text{CH}_3\text{COO})_2\cdot\text{H}_2\text{O}$ –NIPA–melamine were taken in the mole ratio 0.4:0.3:0.3, and the final volume for the reaction was made up to 1.5 mL by the addition of water. The reaction mixtures were stirred for 30 min for homogenization prior to the experiment. The sealed multiclave was placed in a preheated oven at 125 °C for 3 days. After the reaction, the products were recovered by filtration and washed with water under vacuum. The products were analyzed by powder X-ray diffraction (XRD).

The powder XRD patterns of the products indicated the possibility of obtaining hitherto unknown compounds. To optimize the conditions and to synthesize larger quantities of the sample, required for the full characterization, the conventional hydrothermal method was subsequently employed. The hydrothermal method, indeed, was successful and yielded good quality single crystalline products, which are designated as compounds **I**, **II**, and **III**. The additional products, identified during the HT experiments, designated **IIa**, **IIIa**, and **IIIb**, could be obtained only as polycrystalline fine powders.

For the conventional hydrothermal preparation of **I**, $\text{Cu}(\text{CH}_3\text{COO})_2\cdot\text{H}_2\text{O}$ (0.079 g, 0.4 mM) was dissolved in 10 mL of water. To this, 5-nitroisophthalic acid (0.084 g, 0.4 mM) and melamine

(0.038 g, 0.3 mM) were added under continuous stirring. The mixture was homogenized for 30 min at room temperature. The final mixture was transferred, sealed in a 23 mL PTFE-lined stainless steel autoclave, and heated at 125 °C for 3 days under autogenous pressure. For the preparation of **II**, $\text{Cu}(\text{CH}_3\text{COO})_2\cdot\text{H}_2\text{O}$ (0.118 g, 0.6 mM), 5-nitroisophthalic acid (0.127 g, 0.6 mM), and tetrazole (0.05 mL of 30% tetrazole in acetonitrile) were used. For the preparation of **III**, $\text{Cu}(\text{CH}_3\text{COO})_2\cdot\text{H}_2\text{O}$ (0.079 g, 0.4 mM), 5-nitroisophthalic acid (0.063 g, 0.3 mM), and aminotetrazole (0.026 g, 0.3 mM) were employed. During the preparation of compounds **II** and **III**, all of the other synthetic conditions were kept similar to that followed for **I**. The final products contained large quantities of green block (**I**), blue rod (**II**), and blue rod (**III**) type single crystals, were filtered under vacuum, were washed with deionized water, and were dried at ambient conditions.

Initial characterizations were carried out by elemental analysis, powder XRD, thermogravimetric analysis (TGA), and infrared (IR) spectroscopic studies. Powder XRD patterns were recorded in the 2θ range 5–50° using Cu Kα radiation (Philips X'pert) (ESI, Supporting Information, Figures S1–S3). The IR spectra for the compounds were recorded as KBr pellets (Perkin-Elmer, Spectrum 1000). The IR spectra exhibited typical peaks corresponding to the hydroxyl group, amino group, nitro group, and carboxylate groups of the compounds (ESI, Supporting Information, Figure S4). IR (KBr): $\gamma_{\text{as}}(\text{O}-\text{H}) = 3460\text{--}3597 \text{ cm}^{-1}$, $\gamma_s(\text{N}-\text{H}) = 3152\text{--}3455 \text{ cm}^{-1}$, $\gamma_s(\text{C}-\text{H})_{\text{aromatic}} = 2927\text{--}3085 \text{ cm}^{-1}$, $\gamma_s(\text{C}=\text{O}) = 1597\text{--}1618 \text{ cm}^{-1}$, $\delta(\text{H}_2\text{O}) = 1540\text{--}1569 \text{ cm}^{-1}$, $\delta(\text{COO}) = 1432\text{--}1438 \text{ cm}^{-1}$, $\gamma_s(\text{N}-\text{O}) = 1352\text{--}1390 \text{ cm}^{-1}$, $\gamma_s(\text{C}-\text{C})_{\text{skeletal}} = 1074\text{--}1082 \text{ cm}^{-1}$, $\delta(\text{CN})_{\text{skeletal}} = 904\text{--}926 \text{ cm}^{-1}$, and $\delta(\text{CH}_{\text{aromatic}})_{\text{out of plane}} = 767\text{--}788 \text{ cm}^{-1}$ (Supporting Information, Table S1). Elemental analysis: Anal. calcd for **I**: C, 34.32; H, 1.59; N, 13.35. Found: C, 34.18; H, 1.95; N, 13.89. Anal. calcd for **II**: C, 22.70; H, 1.89; N, 14.73. Found: C, 23.08; H, 2.11; N, 14.22. Anal. calcd for **III**: C, 22.11; H, 2.25; N, 17.20. Found: C, 22.68; H, 2.73; N, 16.89. Anal. calcd for **IIa**: C, 25.54; H, 1.43; N, 16.55. Found: C, 26.08; H, 2.31; N, 16.89. Anal. calcd for **IIIa**: C, 25.72; H, 1.20; N, 19.99. Found: C, 26.16; H, 2.4; N, 28.07. Anal. calcd for **IIIb**: C, 22.21; H, 2.05; N, 28.52. Found: C, 22.93; H, 2.71; N, 28.07.

Single Crystal Structure Determination. A suitable single crystal of each compound was carefully selected under a polarizing microscope and glued to a thin glass fiber. The single crystal data were collected on a Bruker AXS smart Apex CCD diffractometer at 293(2) K. The X-ray generator was operated at 50 kV and 35 mA using Mo Kα ($\lambda = 0.71073 \text{ \AA}$) radiation. Data were collected with ω scan width of 0.3°. A total of 606 frames were collected in three different setting of φ (0, 90, and 180°) keeping the sample-to-detector distance fixed at 6.03 cm and the detector position (2θ) fixed at –25°. The data were reduced using SAINTPLUS,¹³ and an empirical absorption correction was applied using the SADABS program.¹⁴ The structure was solved and refined using SHELXL97¹⁵ present in the WinGx suit of programs (Version 1.63.04a).¹⁶ The hydrogen position of the $\mu_3\text{-OH}$ groups and the water molecules in compounds **II** and **III** could not be located from the difference Fourier maps. The possible hydrogen positions were arrived based on the bond valence sum (BVS) calculations for the $\mu_3\text{-OH}$ group.¹⁷ All of the other hydrogen positions were initially located from the difference Fourier maps, and for the final refinement, the hydrogen atoms were placed in geometrically ideal positions and refined in the riding mode. Final refinement included atomic positions for all of the atoms, anisotropic thermal parameters for all of the nonhydrogen atoms, and isotropic thermal parameters for all of the hydrogen atoms. Full-matrix least-squares refinement against $|F^2|$ was carried out using the WinGx package of programs.¹⁵ Details of the structure solution and final refinements for the compounds are given in Table 1. CCDC 792141–792143 contains the crystallographic data for the compounds. These data can be obtained free of charge from The Cambridge Crystallographic Data Center (CCDC) via www.ccdc.cam.ac.uk/data_request/cif.

Table 1. Crystal Data and Structure Refinement Parameters for Compounds I–III^a

	I	II	III
empirical formula	[Cu ₃ {(NO ₂)—C ₆ H ₃ —(COO) ₂ } ₃ (C ₃ N ₆ H ₆)]	[Cu ₂ (μ ₃ -OH)(H ₂ O){(NO ₂)—C ₆ H ₃ —(COO) ₂ }—(CN ₄ H)]·(H ₂ O)	[Cu ₂ (μ ₃ -OH)(H ₂ O){(NO ₂)—C ₆ H ₃ —(COO) ₂ }—(CN ₅ H ₂)]·2(H ₂ O)
formula weight	944.10	476.26	488.27
crystal system	trigonal	monoclinic	orthorhombic
space group	R <bar{3}< td=""><td>P2(1)/m</td><td>P2(1)2(1)2(1)</td></bar{3}<>	P2(1)/m	P2(1)2(1)2(1)
<i>a</i> (Å)	16.3706(8)	10.0134(2)	6.4094(15)
<i>b</i> (Å)	16.3706(8)	6.5861(2)	14.857(4)
<i>c</i> (Å)	22.5362(14)	11.4842(3)	16.066(5)
α (°)	90	90	90
β (°)	90	90.144(2)	90
γ (°)	120	90	90
volume (Å ³)	5230.5(5)	757.37(3)	1529.8(7)
<i>Z</i>	18	4	4
<i>T</i> (K)	293(2)	293(2)	293(2)
ρ _{calcd} (g cm ⁻³)	1.798	2.062	2.103
μ (mm ⁻¹)	1.907	2.876	2.852
θ range (deg)	2.49–25.99	2.70–25.98	1.87–24.59
λ (Mo Kα) (Å)	0.71073	0.71073	0.71073
<i>R</i> _{int}	0.0326	0.0308	0.0506
reflection collected	11645	4640	6264
unique reflections	2277	1619	2533
no. of parameters	172	151	244
<i>R</i> indices [<i>I</i> > 2σ(<i>I</i>)]	<i>R</i> ₁ = 0.0278, <i>wR</i> ₂ = 0.0837	<i>R</i> ₁ = 0.0499, <i>wR</i> ₂ = 0.1183	<i>R</i> ₁ = 0.0490, <i>wR</i> ₂ = 0.1113
<i>R</i> indices (all data)	<i>R</i> ₁ = 0.0330, <i>wR</i> ₂ = 0.0850	<i>R</i> ₁ = 0.0591, <i>wR</i> ₂ = 0.1204	<i>R</i> ₁ = 0.0656, <i>wR</i> ₂ = 0.1216

^a $R_1 = \sum|F_o - |F_c||/\sum|F_o|$; $wR_2 = \{\sum[w(F_o^2 - F_c^2)]/\sum[w(F_o^2)]\}^{1/2}$; $w = 1/[\rho^2(F_o)^2 + (aP)^2 + bP]$; $P = [\max(F_o, O) + 2(F_c)^2]/3$, where $a = 0.0565$ and $b = 0.0000$ for I, where $a = 0.0239$ and $b = 3.9139$ for II, and where $a = 0.0516$ and $b = 3.5074$ for III.

Heterogeneous Catalytic Studies. The reagents required for the heterogeneous catalytic cyanosilylation studies, *N*-benzilidine aniline and trimethylsilyl cyanide (Aldrich), were used as received. The reagents were taken in a 100 mL round-bottom flask with the freshly distilled dichloromethane (DCM) solvent. After the addition of the solid catalyst (copper nitroisophthalate), the mixture was stirred for 6 h at 0 °C in N₂ atmosphere. The product was filtered through Millipore membrane filters to remove the catalyst particles. The supernatant liquid was dried under vacuum to remove the solvent. The product was analyzed and evaluated for the conversion of the reactants.

HT Studies. The system, Cu(CH₃COO)₂·H₂O–NIPA–heterocyclic ligand (melamine/tetrazole/aminotetrazole)–H₂O, was explored employing a HT screening method. The products were characterized by powder XRD, which suggested the possibility of the formation of six new phases. Of these, three compounds (I–III) were subsequently prepared as single crystalline product by employing the conventional hydrothermal method. The other three compounds IIa, IIIa, and IIIb were isolated only as microcrystalline products and were characterized in detail using a variety of techniques. The possible lattice parameters for compounds IIa, IIIa, and IIIb were obtained by the Le Bail fit of the observed powder XRD pattern. The following are the trends observed with regard to the composition and temperature of the reactions under the HT conditions. The HT study of the melamine system indicated that the compound appears to form as a single phase. An unknown phase, however, appears to form both at high and at low melamine concentrations. The stability of compound I decreased with either the increase or the decrease in the temperature of the reaction (Figure 1). The reaction involving the tetrazole ligand indicated that the most stable phase is compound IIa.

The compound II, whose structure is determined as part of this study, appears to form only in a narrow compositional range, and a single phase of II can be isolated only at a low NIPA concentration at 125 °C. The compound IIa forms only as microcrystalline powder throughout the scanned compositional range (ESI, Supporting Information, Figure S5). The reactions with aminotetrazole as the ligand indicated the formation of three distinct phases. Of these, compound III appears to be the stable phase and can be isolated as a single crystalline compound over a wide compositional range at 125 °C. At low NIPA concentration, compound IIIa forms as a microcrystalline powder at 75 and 125 °C. A new phase, compound IIIb, appears to form at 150 °C as a microcrystalline powder (ESI, Supporting Information, Figure S6). The microcrystalline phases IIa, IIIa, and IIIb were indexed, and the unit cell parameters were obtained from the powder XRD patterns by the Le Bail method¹⁸ (ESI, Supporting Information, Figures S7–S9 and Table S3). The possible compositions of these were obtained by correlating a variety of techniques. Thus, elemental analysis, TGA, and IR spectroscopic studies were employed to arrive at the molecular formula for the compounds IIa, IIIa, and IIIb. The possible molecular formulas were found to be Cu₂{(NO₂)—C₆H₃—(COO)₂}(CN₄H)(H₂O) for IIa, Cu₂{(NO₂)—C₆H₃—(COO)₂}—(CN₅H₂) for IIIa, and Cu₂{(NO₂)—C₆H₃—(COO)₂}—(CN₅H₂)₂2H₂O for IIIb. Although the molecular formulas of IIa, IIIa, and IIIb are comparable to the present compounds II and III, the bonding between the metal centers and the ligands (NIPA and tetrazole/aminotetrazole) is still not known, and one could possibly consider them as polymorphic/related phases. Our efforts to isolate these compounds as single crystalline products were not successful.

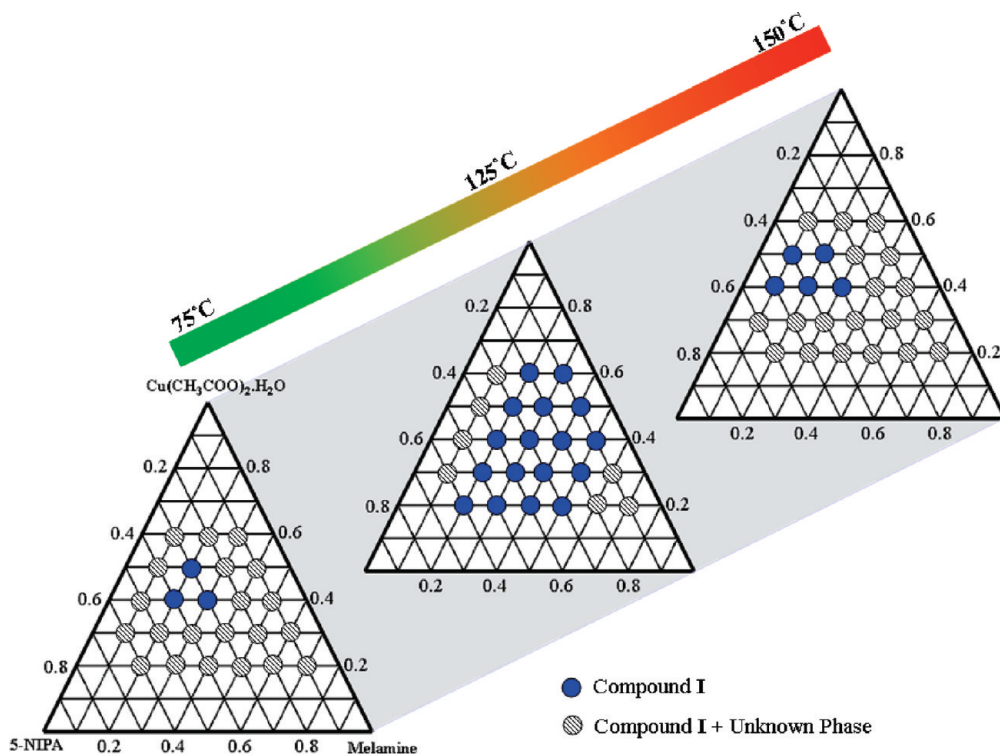


Figure 1. (a) Summary of the HT screening of the Cu/NIPA/melamine system as a function of reactant concentration and temperature. The results presented are based on the analysis of the PXRD studies.

Table 2. Selected Observed Bond Distances in the Compounds I–III^a

bond	distances (Å)	bond	distances (Å)	bond	distances (Å)
I					
Cu(1)–O(1)#1	1.9619(16)	Cu(1)–O(2)#2	1.9621(16)	Cu(1)–O(3)#3	1.9683(16)
Cu(1)–O(4)	1.9762(16)	Cu(1)–N(1)	2.2560(18)		
II					
Cu(1)–O(1)#1	1.903(6)	Cu(1)–N(1)#2	2.196(5)	Cu(2)–O(8)#4	2.479(8)
Cu(1)–O(2)	2.000(5)	Cu(1)–N(1)	2.196(5)	Cu(2)–O(8)	2.479(8)
Cu(1)–O(3)	2.206(6)	Cu(2)–O(3)#3	1.951(3)	Cu(2)–N(2)	1.992(5)
Cu(1)–O(4)	2.279(7)	Cu(2)–O(3)	1.951(3)	Cu(2)–N(2)#3	1.992(5)
III					
Cu(1)–O(1)	1.911(5)	Cu(1)–N(2)#2	2.093(8)	Cu(2)–O(5)	2.239(7)
Cu(1)–O(2)#1	1.993(5)	Cu(1)–N(1)	2.104(7)	Cu(2)–N(3)#4	1.981(8)
Cu(1)–O(3)	2.313(5)	Cu(2)–O(3)#3	1.935(7)	Cu(2)–N(4)	2.001(8)
Cu(1)–O(4)#1	2.433(5)	Cu(2)–O(3)	1.938(7)		

^a Symmetry transformations used to generate equivalent atoms: I: #1, -x, -y + 1, -z; #2, -y + 2/3, x - y + 4/3, z + 1/3; #3, y - 2/3, -x + y - 1/3, -z - 1/3. II: #1, x + 1, y, z; #2, x, -y + 5/2, z; #3, -x + 2, -y + 2, -z + 2; #4, x, y, z. III: #1, -x + 1/2, -y + 1, z + 1/2; #2, x + 1, y, z; #3, x - 1/2, -y + 1/2, -z + 1; #4, x + 1/2, -y + 1/2, -z + 1.

RESULTS

Structure of $[\text{Cu}_3\{(\text{NO}_2)-\text{C}_6\text{H}_3-(\text{COO})_2\}_3(\text{C}_3\text{N}_6\text{H}_6)]$ (I). The asymmetric unit of $[\text{Cu}_3\{(\text{NO}_2)-\text{C}_6\text{H}_3-(\text{COO})_2\}_3(\text{C}_3\text{N}_6\text{H}_6)]$ (I) consists of 19 nonhydrogen atoms. One Cu^{2+} ion, one NIPA, and one-third of a melamine molecule contribute to the asymmetric unit (ESI, Supporting Information, Figure S10). The Cu^{2+} ions are coordinated with four carboxylate oxygen atoms and one nitrogen atom from melamine, forming a distorted square pyramidal geometry (CuO_4N). The $\text{Cu}-\text{O}$ bonds have distances in the range of

1.962(2)–1.976(2) Å (average, 1.967 Å), and the $\text{Cu}-\text{N}$ bond distance is 2.256(2) Å for I (Table 2).

The structure of I consists of connectivity between the copper centers, the melamine, and the nitroisophthalate. Each of the carboxylate oxygens of the 5-nitroisophthalic acid is bonded to one copper atom and has monodentate connectivity (ESI, Supporting Information, Figure S11). The nitro group does not participate in bonding in the structure. The connectivity between the copper and the carboxylate group gives rise to the paddle wheel unit (ESI, Supporting Information, Figure S12).

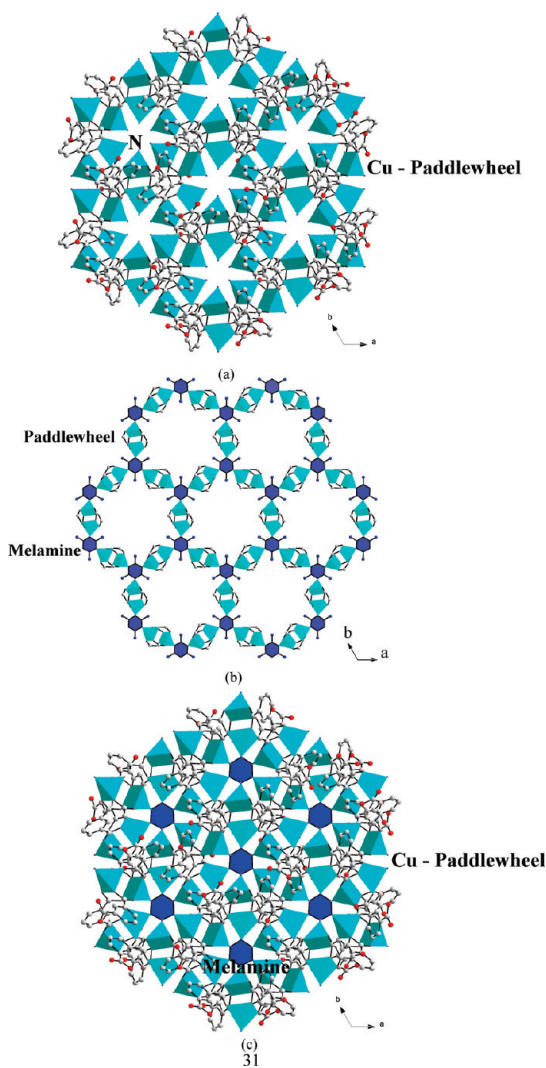


Figure 2. (a) Figure shows the connectivity between the paddle wheel copper centers and the nitroisophthalate (NIPA) forming the three-dimensional structure in $[Cu_3\{(NO_2)-C_6H_3-(COO)_2\}_3-(C_3N_6H_6)\}$ (**I**). (b) View of the two-dimensional layer formed by the connectivity between the copper paddle wheels and the melamine. (c) The overall view of three-dimensional structure of **I**. Note that the melamine units occupy the middle of the channels formed by Cu–NIPA connectivity.

The paddle wheel is one of the fundamental building units in the family of MOFs and has been routinely observed in compounds containing copper.¹⁹ The connectivity between the copper paddle wheels and the acid gives rise to a three-dimensional structure with one-dimensional channels along the *c*-axis (Figure 2a). The melamine unit also connects three such paddle wheels through the Cu–N bonds (ESI, Supporting Information, Figure S13), forming a two-dimensional layer in the *ab* plane (Figure 2b). It may be noted that the Cu–NIPA as well as the Cu–melamine connectivity exhibit the 3-fold symmetry, which is typical of the space group ($R\bar{3}$). Interconnectivity between the Cu–NIPA and the Cu–melamine units is such that the melamine units occupy the middle of the one-dimensional channels, which renders the channels inaccessible (Figure 2c). The terminal amino group of the melamine molecules participates in N–H \cdots O hydrogen bonds. The N \cdots O distances of 2.822 and

3.342 Å and the N–H \cdots O bond angles of 157 and 151° observed in **I** suggest that these interactions are not very strong.²⁰

Structure of $[Cu_2(\mu_3-OH)(H_2O)\{(NO_2)-C_6H_3-(COO)_2\}(CN_4H)\}\cdot(H_2O)$ (II**)**. The asymmetric unit of $[Cu_2(\mu_3-OH)(H_2O)\{(NO_2)-C_6H_3-(COO)_2\}(CN_4H)\]\cdot(H_2O)$ (**II**) consists of 25 nonhydrogen atoms. Two crystallographically independent Cu^{2+} ions along with one NIPA anion, one tetrazolate, one μ_3 -hydroxyl group, one coordinated water molecule, and one lattice water molecule contribute to the asymmetric unit (ESI, Supporting Information, Figure S14). Both of the Cu^{2+} ions have distorted octahedral coordination; $Cu(1)$ is coordinated by one μ_3 hydroxyl ion [$O(3)$], three carboxylate oxygens, and two nitrogens from the tetrazolate ligand, forming $Cu(OH)O_3N_2$ octahedra, and $Cu(2)$ is coordinated by two μ_3 -hydroxyl ion [$O(3)$ and $O(3)^*$], two aqua oxygens, and two triazolate nitrogens to form a $Cu(OH)_2(H_2O)_2N_2$ octahedra. The Cu–O bonds have distances in the range 1.903(6)–2.479(8) Å (average, 2.156 Å), and the Cu–N bonds have distances in the range 1.992(5)–2.196(5) Å (average, 2.094 Å) for **II** (Table 2).

The structure of **II** can be understood by considering the independent connectivity between the metal centers with tetrazole and NIPA. The two carboxylate groups of the NIPA connect to two copper centers with one monodentate and one bidentate coordination mode (ESI, Supporting Information, Figure S15). The connectivity between the NIPA and the copper centers results in the formation of a one-dimensional chain structure (Figure 3a). The copper atoms themselves are connected through μ_3 -hydroxyl group forming an infinite one-dimensional zigzag Cu–O(H)–Cu chain, which lies along the 2_1 axis. The tetrazolate units occupy the grooves in the zigzag (helical) chain and bond with four copper centers (ESI, Supporting Information, Figure S16), giving rise to a one-dimensional ladderlike structure. The copper atoms are arranged in a triangular manner connected through the corners (Figure 3b). The copper–tetrazolate ladders and the copper–nitroisophthalate chains are connected together in such way that they are mutually orthogonal to each other forming a two-dimensional bilayer arrangement. The layers are arranged in such a way to give rise to a pseudo three-dimensional structure encompassing a one-dimensional channel of width 6.8 Å × 8.9 Å (shortest atom–atom contact distances, not including the van der Waals radii) (Figure 3c). The coordinated water molecules from the copper center project into the middle of the channels. The bilayers are arranged in a AAA \cdots fashion (Figure 3d).

Structure of $[Cu_2(\mu_3-OH)(H_2O)\{(NO_2)-C_6H_3-(COO)_2\}(CN_5H_2)\}\cdot2(H_2O)$ (III**)**. The asymmetric unit of $[Cu_2(\mu_3-OH)(H_2O)\{(NO_2)-C_6H_3-(COO)_2\}(CN_5H_2)\]\cdot2(H_2O)$ (**III**) consists of 27 nonhydrogen atoms. Two crystallographically independent Cu^{2+} ions, one NIPA anion, one aminotetrazolate ligand, one μ_3 -hydroxyl group, one coordinated water molecule, and two lattice water molecules constitute the asymmetric unit (ESI, Supporting Information, Figure S17). Of the two copper atoms, $Cu(1)$ is octahedrally coordinated by one μ_3 hydroxyl ion [$O(3)$], three carboxylate oxygens, and two nitrogens from the aminotetrazolate, forming a $Cu(OH)O_3N_2$ unit, and $Cu(2)$ is coordinated by two μ_3 -hydroxyl ion [$O(3)$ and $O(3)^*$], two nitrogens from the aminotetrazole molecule, and one aqua oxygen to form a $Cu(OH)_2(H_2O)N_2$ distorted trigonal bipyramidal geometry. The Cu–O bonds have distances in the range 1.911(5)–2.433(5) Å (average, 2.109 Å) and the Cu–N bond distances in the range of 1.981(8)–2.104(7) Å (average, 2.045 Å) (Table 2).

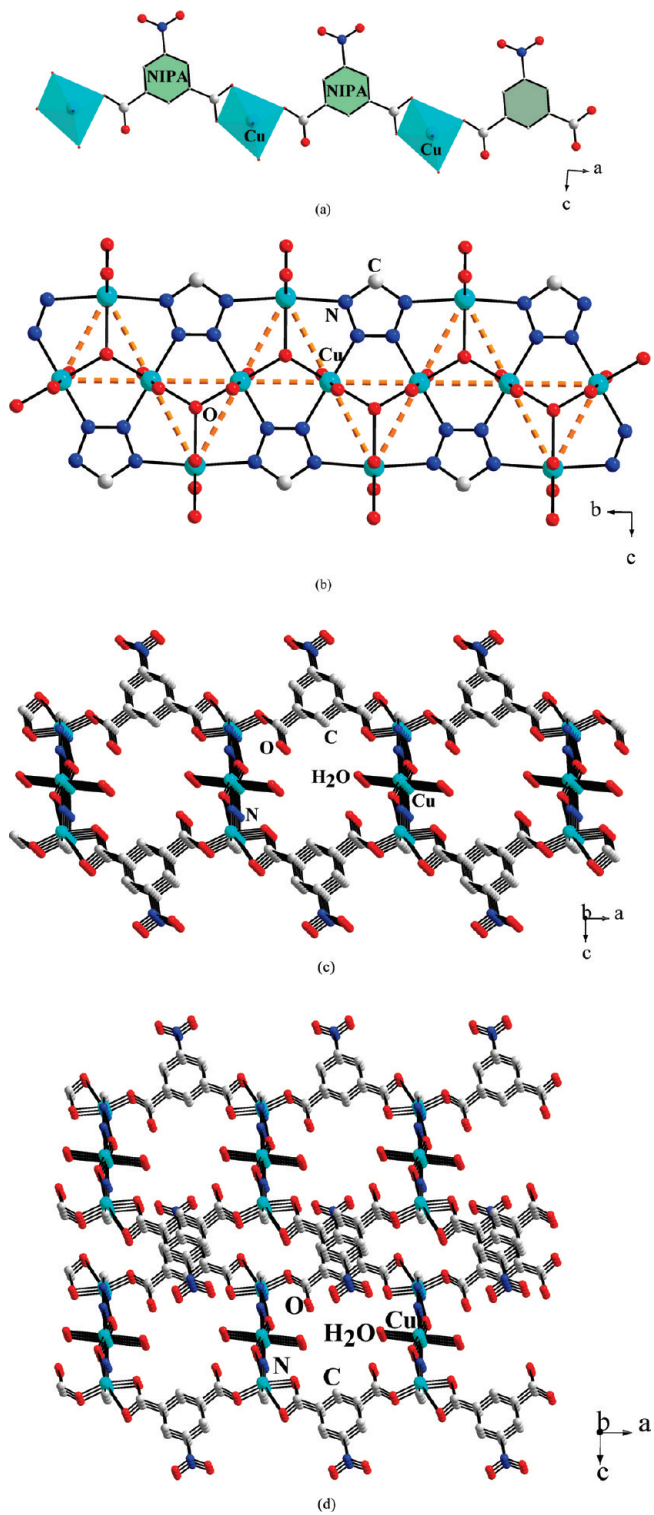


Figure 3. (a) One-dimensional chain formed by the connectivity between copper and NIPA in $[\text{Cu}_2(\mu_3\text{-OH})(\text{H}_2\text{O})\{(\text{NO}_2)_2\text{-C}_6\text{H}_3\text{-(COO)}_2\}(\text{CN}_4\text{H})]\cdot 2(\text{H}_2\text{O})$ (**II**). (b) View of the one-dimensional ladderlike structure formed by the connectivity between copper and tetrazolate. (c) View of the two-dimensional layer in the *ac* plane formed by the connectivity between the copper–NIPA chains and the copper–tetrazolate ladders. Note the orthogonal arrangement of the two one-dimensional units (see the text). (d) View of the arrangement of the layers in **II**. Note the formation of the three-dimensional-like structure through supramolecular interactions.

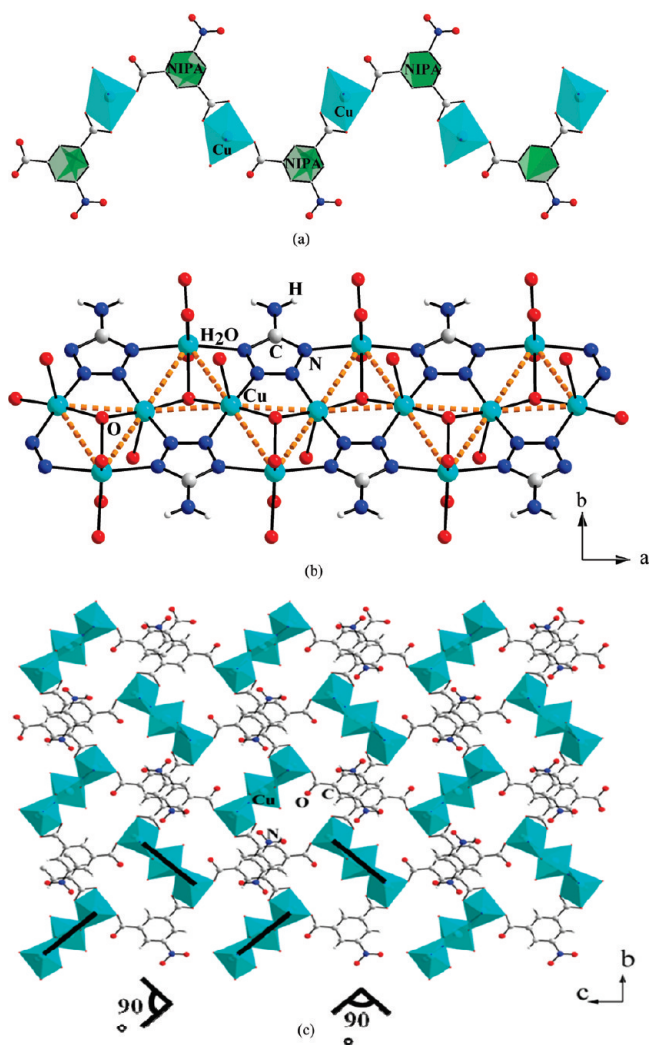


Figure 4. (a) One-dimensional zigzag chain formed by the connectivity between copper and NIPA in $[\text{Cu}_2(\mu_3\text{-OH})(\text{H}_2\text{O})\{(\text{NO}_2)_2\text{-C}_6\text{H}_3\text{-(COO)}_2\}(\text{CN}_4\text{H})]\cdot 2(\text{H}_2\text{O})$ (**III**). (b) View of the one-dimensional ladderlike structure formed by the connectivity between copper and aminotetrazolate. Note the similarity with the structure in **II** (Figure 3b). (c) View of the three-dimensional structure of **III** formed by the connectivity between the copper–NIPA chains and copper–aminotetrazolate ladders. Note the orthogonal arrangement of the copper–aminotetrazolate ladders (see the text).

The structure of **III** is closely related to the structure of **II**. The two carboxylate groups of the NIPA unit connect with two copper centers with one monodentate and one bis-bidentate coordination mode (ESI, Supporting Information, Figure S18). The connectivity between the NIPA with the copper center results in a one-dimensional structure, which is similar to that observed in **II** (Figure 4a). The μ_3 -hydroxyl groups connect the copper atoms, forming an infinite one-dimensional zigzag $\text{Cu}-\text{O}(\text{H})-\text{Cu}$ chain as in **II**, with a corner shared triangular arrangement. The aminotetrazole unit occupies the spaces in between the copper atoms, forming a one-dimensional ladderlike arrangement (Figure 4b). The ladders are positioned in such a way that they are orthogonal to each other (Figure 4c). The copper–nitroisophthalate chains and the copper–aminotetrazolate ladders are connected together, forming the three-dimensional structure (Figure 4c).

■ DISCUSSION

A HT screening method has been employed for the identification of the formation of new phases in Cu–NIPA–heterocyclic ligand systems. We have been able to obtain one single crystalline product with melamine as the ligand (compound I). From the phase diagram (Figure 1), it is clear that this phase forms over a wide compositional range at 125 °C, whereas the formation of I is limited at low (75 °C) as well as at higher temperature (150 °C). In the case of the tetrazolate ligand, the identified compound (II) forms in a very narrow concentration range, and the stability of II also appears to be sensitive to the variation in the temperature. The phase diagram of the reaction mixture involving aminotetrazole as the ligand appears to be even more complex. We have identified three phases of which one was isolated as a single crystalline phase (III), whereas two other phases (designated as IIIa and IIIb) form as a microcrystalline powder. We observed that the stabilities of the phase III appear to be low at low (75 °C) as well as at high (150 °C) temperatures.

From the structural point of view, the three compounds I–III are formed through the coordination of nitroisophthalate and heterocyclic ligand with the copper atoms. Compound I is different from II and III as it is formed with a copper paddle wheel structure, whereas II and III have similar one-dimensional –Cu–O(H)–Cu– connectivity. The structural formula and the asymmetric unit of compound II and III show that they differ only by one lattice water molecule. The connectivity between the tetrazole (II) and the aminotetrazole (III) units with the copper centers is the same, and also, the connectivity between the carboxylate groups and the copper is similar between the two structures II and III. However, both of the structures differ in the overall dimensionality. While compound II has a two-dimensional layer structure, compound III has a three-dimensional structure. This can be understood by a closer look at the connectivity of the one-dimensional ladders formed between the copper and the azaheterocycles (tetrazole and aminotetrazole) with the NIPA. In structure II, the NIPA links the adjacent ladders, forming the two-dimensional layer structure; the NIPA and the copper tetrazole ladders are similar, being stacked one above the other (Figure 5a). In III, the connectivity between the NIPA and the copper aminotetrazole is different. The Cu–aminotetrazole ladders are not arranged parallel to each other but are arranged orthogonal to each other (Figure 4c). This subtle difference in the connectivity between the structures of II and III is responsible for the dimensionality differences. The NIPA units, thus, connect the ladders in such a way that it forms a three-dimensional structure (Figure 5b).

The staking of the two-dimensional layers of compound II is also stabilized by the π – π interaction between the nitroisophthalate anions. The role of π – π interactions in the formation of the supramolecular compounds is a topic of interest and is well documented.²¹ In compound II, we find significant intra-layer π – π /CH \cdots π interactions between the aromatic rings of the nitroisophthalate anions (Figure 6). To understand the nature and the energies involved in these interactions, we performed calculations using Gaussian98 software package at the B3LYP/6-31+G(d,p) level.²² The calculated energies for the

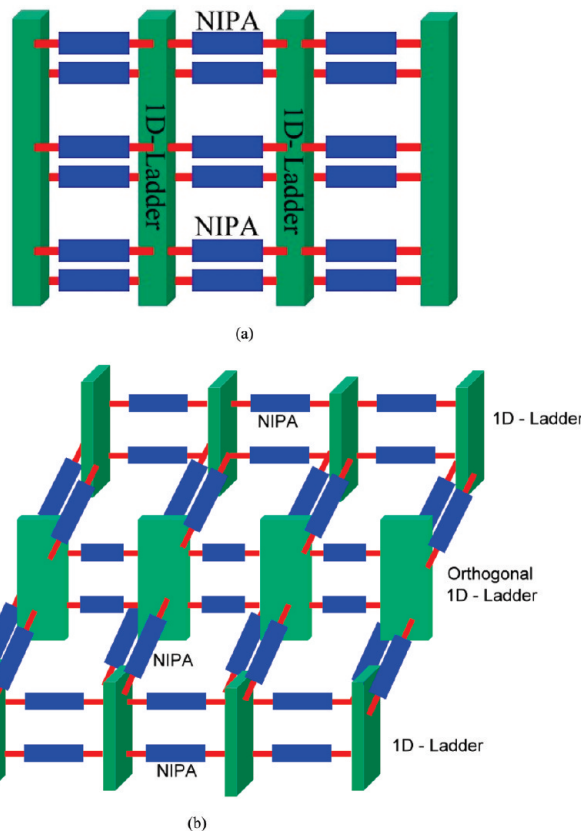


Figure 5. (a) Schematic representation of the connectivity observed in II. (b) Schematic representation of the connectivity observed in III. Note the differences in the connectivity, which leads to a 3D structure (see the text).

interaction between the benzene rings were 1.66 kcal mol⁻¹. The values observed are similar to the π – π interaction energies observed before.²³ The nitroisophthalate units in the structure of III are far apart (\sim 6.5 Å) from each other to have any meaningful π – π /CH \cdots π interactions.

Thermogravimetric Studies. TGA on the compounds has been carried out in flowing air (flow rate = 20 mL min⁻¹) in the temperature range 30–800 °C (heating rate = 5 °C min⁻¹). The TGA studies indicate that compound I exhibits a single-step weight loss. The total observed weight loss of 74% in the temperature range 280–350 °C corresponds to the loss of all of the carboxylate and the melamine units (calcd, 74.7%). Compound II exhibits an initial weight loss of \sim 7.5% below 100 °C, which may be due to the loss of the lattice and the coordinated water molecules (calcd, 9.2%) and the second weight loss of 57% in the temperature range 290–310 °C, which would correspond to the loss of the carboxylate and the tetrazolate moieties. The total observed weight loss of 64.5% compares well with the loss of all of the water molecules (coordinated and lattice), the tetrazolate, and the carboxylate units (calcd, 66.6%). Compound III also exhibits a similar behavior with losses of \sim 8.5% up to 130 °C and 61% in the range 260–275 °C. The total observed weight loss of 69.5% corresponds well with the loss of the carboxylate, the aminotetrazolate, and all of the water molecules (calcd, 67.4%) (ESI, Supporting Information, Figure S19). The final calcined products in all of the cases was found to be crystalline and corresponds to CuO (JCPDS: 80-1916).

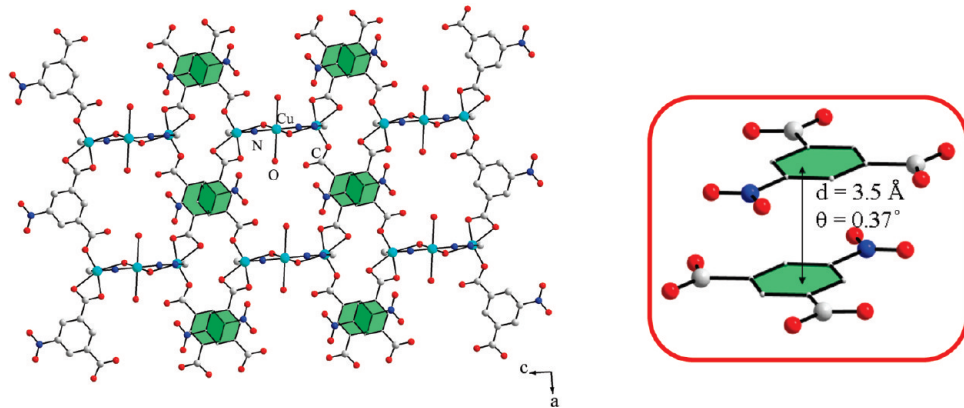


Figure 6. Stacking of the layers in **II**. The $\pi-\pi$ interactions are shown in the inset.

We have also carried out the thermal studies on the micro-crystalline powdered samples **IIa**, **IIIa**, and **IIIb** to understand the thermal stabilities. The TGA studies of compound **IIa** indicate an initial weight loss of $\sim 3.7\%$ up to $150\text{ }^{\circ}\text{C}$, which may be due to the loss of a water molecule (calcd, 4.3%). The second weight loss of $\sim 57.8\%$ near the temperature range of $230\text{--}290\text{ }^{\circ}\text{C}$ may be due to the loss of the carboxylate and the tetrazolate units. The total observed weight loss of 67% nearly compares with the loss of water molecule and the organic moieties (calcd, 67%). Compound **IIIa** exhibits a single-step weight loss with the observed weight loss of $\sim 64\%$ in the temperature range $245\text{--}280\text{ }^{\circ}\text{C}$, which corresponds to the loss of all of the carboxylate and the aminotetrazolate units (calcd, 61.2%). Compound **IIIb** shows an initial weight loss of $\sim 9\%$ up to $125\text{ }^{\circ}\text{C}$ and $\sim 61\%$ in the range $200\text{--}280\text{ }^{\circ}\text{C}$. The total observed weight loss of $\sim 70\%$ corresponds well with the loss of the carboxylate, the aminotetrazolate, and all of the water molecules (calcd, 69.8%) (ESI, Supporting Information, Figure S20). The final calcined product in all of the cases was found to be crystalline by powder XRD and corresponds to CuO (JCPDS: 80-1916). We have employed TGA, IR, and the elemental analysis as a means of identifying the probable molecular formula in the case of **IIa**, **IIIa**, and **IIIb**. As can be noted, the weight loss in these compounds (**IIa** and **IIIb**) is also comparable with the losses observed for compounds **II** and **III**. It is likely that the structures could also be comparable. The Le Bail fit of the PXRD patterns of the compounds **IIa**, **IIIa**, and **IIIb** gave lattice parameters (ESI, Supporting Information, Table S3), which are also comparable to the present compounds. We believe that the unknown compounds are likely to have structures that are comparable to the ones reported here.

UV–Visible Spectroscopic Studies. All three compounds isolated in single crystalline form in the present study are colored. The diffuse reflectance UV–vis spectra were measured at room temperature for the as-synthesized compounds along with the NIPA anion (Na salt of NIPA), melamine, and aminotetrazole (ESI, Supporting Information, Figures S21 and S22). The Na-NIPA exhibited two main absorption peaks centered at ~ 330 and $\sim 390\text{ nm}$, melamine has two main peaks at ~ 285 and $\sim 315\text{ nm}$, and aminotetrazole has peaks at ~ 200 , ~ 285 , and $\sim 320\text{ nm}$. The UV–vis spectrum of the tetrazole (30% in acetonitrile) was recorded in the solution phase, which exhibits a main peak at $\sim 225\text{ nm}$. All of these peaks are due to the intraligand charge transfer transitions and appear as a broad peak in all of the compounds. In addition, a broad absorption band in

the range $500\text{--}1000\text{ nm}$ was also observed in all three compounds. This band may be due to the d–d transition of the Cu^{2+} ions. Similar absorption bands have been observed earlier.²⁴

Dynamics of the Water Molecules. *Thermal Studies.* Compounds **II** and **III** have coordinated as well as lattice water molecules. The TGA studies clearly indicated that the water molecules are lost below $\sim 150\text{ }^{\circ}\text{C}$, which prompted us to examine the possible removal and readorption of the water molecules. To investigate the reversible adsorption behavior, a modified TGA set up with a port for introducing the water vapor was employed. A sample of each compound (**II** and **III**) was taken in the TGA crucible and heated to the temperature of complete dehydration in an atmosphere of flowing dry nitrogen (20 mL/min) ($125\text{ }^{\circ}\text{C}$ for **II** and $140\text{ }^{\circ}\text{C}$ for **III**) using a heating rate of $5\text{ }^{\circ}\text{C}/\text{min}$. The samples were cooled slowly to room temperature with a cooling rate of $2\text{ }^{\circ}\text{C}/\text{min}$. To study the rehydration behavior of the compounds, saturated water vapor was introduced at room temperature into the system for 60 min. During the rehydration step, we observed that both compounds **II** and **III** reabsorb the water molecules quickly and reach almost the original weights taken at the start of the dehydration cycle. Thus, 97.5 and 99% of the initial weight were observed from the dehydrated weights of 91.7 and 90% for **II** and **III**, respectively. We also noted that both of the compounds reabsorbed fully ($\sim 100\%$) when kept exposed to atmospheric conditions for a longer duration. Although this trend may be expected, we wanted to examine the recyclability of the dehydration–rehydration behavior. To check the full reversibility, the dehydration and rehydration cycles were repeated twice. We observed that both of the compounds, **II** and **III** (ESI, Supporting Information, Figure S23, and Figure 7), exhibit good recyclability. This observation suggests that the dehydration–rehydration behavior is fully reversible. The powder XRD pattern recorded on the fully rehydrated sample also confirms that the integrity of the original sample is retained (ESI, Supporting Information, Figure S24).

Powder XRD Studies. As the dehydration–hydration cycle is fully reversible, we sought to investigate the structure of the dehydrated phase employing *in situ* single crystal studies. Our efforts were not successful as the dehydrated phase appears to lose the single crystalline nature and did not diffract well under the *in situ* conditions. To probe the crystallinity changes during the dehydration–rehydration cycles, we carried out *ex situ* temperature-dependent powder XRD studies on both compounds **II** and **III**. Powdered samples of **II** and **III** were heated at different temperatures and then examined by powder XRD.

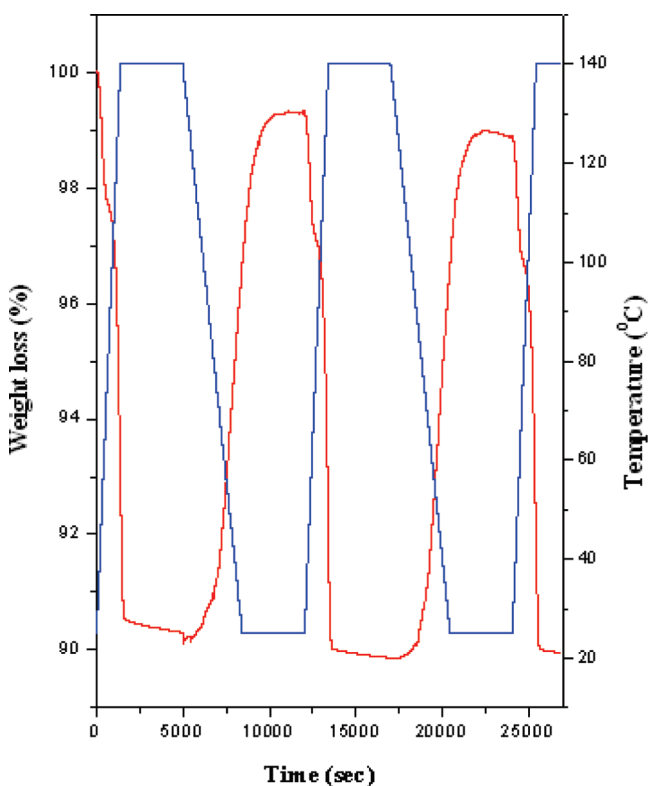


Figure 7. TGA histogram showing the reversible water uptake in compound III. The blue curve represents the heating and the cooling cycle, and the red curve represents the weight loss and weight gain.

The powder XRD pattern of the fully dehydrated phase of **II** (heated at 125 °C for 5 h) indicates a new phase. The original phase reappears when the sample was kept exposed to the atmospheric condition for about 3 h (ESI, Supporting Information, Figure S25). This suggests that the removal of the water molecules (coordinated and lattice) from **II** may be accompanied by a structural reorganization. The powder XRD pattern of **III** heated at 150 °C/5 h indicates a shift of the main peak from $2\theta = 8.1 - 8.25^\circ$. The main peak reverts back toward the original peak position of $2\theta = 8.1^\circ$, when the sample was exposed to the atmospheric condition for 1 h (ESI, Supporting Information, Figure S26). The dehydrated sample of the compound **III** could be fitted using the Le Bail method, which gives the cell parameters for the dehydrated phase (ESI, Supporting Information, Figure S27 and Table S4). As can be noted, the *a* and *b* lattice parameters exhibit a small expansion, whereas *c* exhibits contraction. Similar changes in the lattice parameters during the dehydration have been encountered before.²⁵

IR Spectroscopic Studies. To understand the reversible behavior as well as to examine the possibility of ligand exchanges in **III**, which appears to retain the structural integrity during dehydration, we have carried out IR spectroscopic studies (Perkin-Elmer, SPECTRUM 1000). As part of the ligand exchange studies, we exchanged D₂O in place of H₂O. The IR spectroscopic studies exhibited the normal band for H₂O at $\sim 3500 \text{ cm}^{-1}$. On exchange with D₂O, we observed the appearance of two new bands centered at ~ 2600 and $\sim 2470 \text{ cm}^{-1}$, which would correspond to the coordinated and lattice D₂O stretching vibrations (ESI, Supporting Information, Figure S28).²⁶ This study confirms that the water molecules in **III** are labile and

could be replaced by the D₂O molecules. Similar studies carried out on compound **II** were not successful.

Optical Studies. We wanted to examine the changes that would accompany the removal of water in **II** and **III** using UV-vis studies. Structurally, there are two distinct Cu species in **III**, of which only one has a coordinated water molecule, the removal of which is expected to lead to differences in the primary coordination around the copper. In addition, it is likely that the coordination changes in copper can also lead to changes in color. On dehydration, we observed that the color indeed changes from blue to green. The blue color, of course, returns back after exposure to atmospheric conditions, as expected (ESI, Supporting Information, Figure S29). In addition, the PXRD studies also indicated that the water removal from compound **III** does not disrupt the structural integrity.

To probe this change of color further, compound **III** was heated under vacuum in a glass tube for 5 h at 150 °C, and the green-colored samples were carefully transferred to a quartz sealed cuvette inside a glovebox. The UV-vis spectrum of the dehydrated sample, then, was recorded at room temperature. The UV-vis spectra of the dehydrated sample of compound **III** show two peaks centered at ~ 265 and $\sim 350 \text{ nm}$, which are due to the intraligand transitions of aminotetrazolate and nitroisophthalate. In addition, a broad absorption band in the range of 500–1000 nm was also observed. The broad absorption band exhibits a maximum at around $\sim 850 \text{ nm}$. To investigate the changes that accompany these bands during the rehydration behavior, the UV-vis spectra of the dehydrated sample were studied by exposing the sample to the atmospheric conditions. During the rehydration, the intraligand transition bands did not exhibit any appreciable changes, whereas the nature of the broad absorption bands starts to change as a function of time (ESI, Supporting Information, Figure S30). The center of the broad absorption shifts to $\sim 780 \text{ nm}$ along with a shoulder at $\sim 650 \text{ nm}$. From the available literature on copper-containing compounds, it appears that the octahedral compounds of Cu²⁺ exhibit absorption bands near $\sim 625 \text{ nm}$ (16000 cm^{-1}), which often has a broad tail into the near-IR region. The broad band has generally been assigned to the transitions from d_{xy} , d_z^2 and d_{xz} , d_{yz} pairs to the σ antibonding and half-filled $d_x^2 - d_y^2$ level. The trigonal bipyramidal compounds exhibit peaks centered around 980 (10200 cm^{-1}) and 1220 nm (8200 cm^{-1}). The four-coordinated Cu²⁺ are generally rare and exist in square pyramidal geometry, which gives rise to peaks at 565 (17700 cm^{-1}), 675 (14750 cm^{-1}), and 775 nm (12900 cm^{-1}).²⁷ The complete assignments for all of the observed absorption bands were not possible in compound **III** as both octahedral and trigonal bipyramidal Cu²⁺ centers exist. It is likely that the trigonal bipyramidal Cu²⁺ center changes to a four-coordinated geometry upon dehydration in **III**. The observed resultant band is a mixture of the known transitions of Cu²⁺ in the various coordination environments. This study was also helpful in confirming the reversibility of the water molecules in **III** as the UV-vis bands regenerate during the dehydration-rehydration cycle.

EPR and Magnetic Studies. The X-band EPR spectra of the compounds in the solid state were recorded at room temperature (ESI, Supporting Information, Figure S31–S33). All of the compounds exhibit a single resonance peak centered at $g = 2.125$ (**I**), $g = 2.178$ (**II**), and $g = 2.216$ (**III**), respectively. The EPR signals exhibit a small anisotropy and hyperfine splitting, which are generally expected for this type of solid. The EPR study

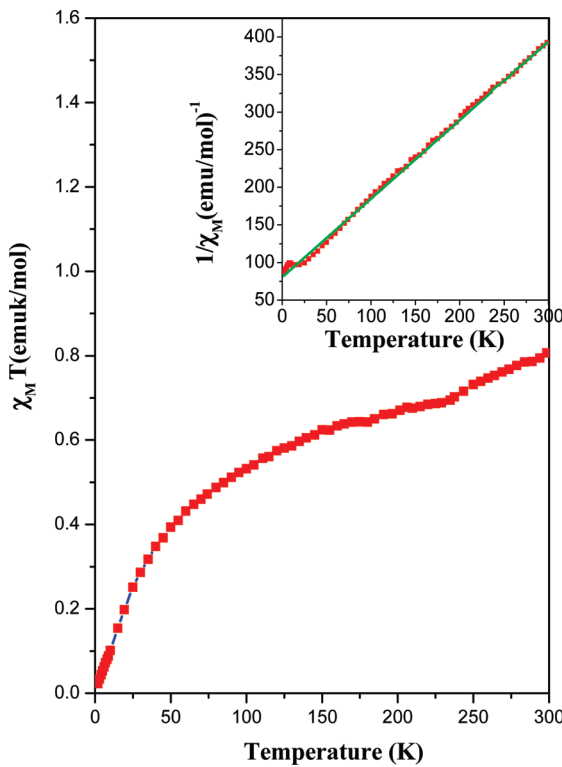


Figure 8. Temperature variation of the $\chi_M T$ for I. The inset shows the corresponding $1/\chi_M$ vs T plots.

confirms that the copper ions in all of the compounds are present in the +2 oxidation state.

Temperature-dependent magnetic susceptibility studies for all three compounds were performed on powdered samples using a SQUID magnetometer (Quantum Design Inc., United States). The $\chi_M T$ value of I decreases slowly from an initial value of 0.80 emu mol⁻¹ K at room temperature to reach a value of 0.023 emu mol⁻¹ K at 2 K (Figure 8). The molar susceptibility, χ_M , value of I increases slowly to reach a maxima at ~ 16 K, which suggests that the onset of long-range order is achieved. The value of χ_M decreases upon cooling further up to 7 K, beyond which it increases sharply again. The sharp increase below 7 K indicates the presence of some paramagnetic impurity. A similar behavior has been observed in compounds containing copper and are known as a Curie tail (Supporting Information, Figure S34).²⁸ A plot of $1/\chi_M$ vs T for the compound I in the temperature range 50–300 K can be fitted to the Curie–Weiss behavior with a value for C of 0.95 emu/mol and θ_P of -76.6 K. The large negative values of θ_P indicate that the dominant exchanges between the copper ions are antiferromagnetic. The large Weiss constant (θ_P) along with high ordering temperature suggests that there is a good overlap between the metal and the oxygen orbitals, leading to strengthened superexchange interactions.

The presence of infinite M–O(H)–M bonds in the compounds II and III along with the triangular arrangement of the copper atoms is expected to give interesting magnetic behavior.²⁹ At room temperature, the $\chi_M T$ values of II and III are 0.71 and 0.77 emu mol⁻¹ K for two Cu²⁺ ions ($\chi_M T = 0.375$ emu mol⁻¹ K for a $S = 1/2$ system, single Cu²⁺ ions), which are close to the value expected for two noncoupled Cu²⁺ ions. The $\chi_M T$ value of II decreases slowly and reaches a minimum of 0.15 emu mol⁻¹ K at 5 K after which it increases marginally (Figure 9). For compound III, the $\chi_M T$ value decreases continuously and reaches a minimum

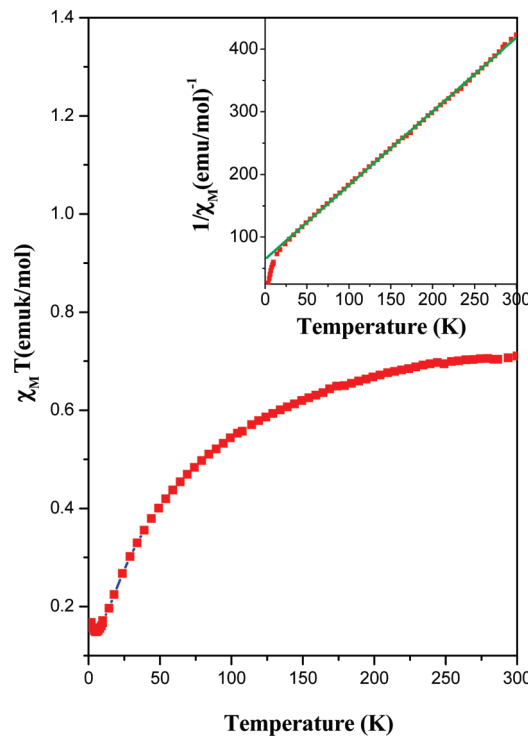


Figure 9. Temperature variation of the $\chi_M T$ for II. The inset shows the corresponding $1/\chi_M$ vs T plots.

of 0.026 emu mol⁻¹ K at 2 K (Figure 10). The molar magnetic susceptibility, χ_M , of II increases very slowly from 0.0024 emu mol⁻¹ at room temperature to a value of 0.0137 at 14 K, after which it exhibits a sharp rise (Supporting Information, Figure S35). A similar behavior was observed for III where the χ_M value increases from 0.0025 emu mol⁻¹ at room temperature to a value of 0.0086 at 14 K, after which it exhibits a sharp increase (Supporting Information, Figure S36). The field-cooled (FC) and zero-field-cooled (ZFC) studies on both of the compounds did not exhibit any appreciable differences in the χ_M behavior up to 2 K (ESI, Supporting Information, Figures S37 and S38). The magnetization studies also did not reveal any possible hysteresis behavior (ESI, Supporting Information, Figures S39 and S40). The present studies indicate that there are no long-range ferromagnetic correlations between the Cu²⁺ ions in both of the compounds, II and III. The $1/\chi_M$ vs T data for compounds II and III can be fitted in the temperature range 50–300 K for the Curie–Weiss behavior, which gave a value for C of 0.848 emu/mol and θ_P of -55 K for II and a value of 1.076 emu/mol for C and $\theta_P = -116.8$ K for III. The very high negative values of θ_P obtained for both II and III again indicate that the magnetic exchanges between the copper centers through the oxygen are strong. Similar large negative θ_P values have been observed in other copper-containing MOF compounds.³⁰

Heterogeneous Catalytic Studies. Single site heterogeneous catalysis is important as it facilitates the correlation of catalytic activity with the crystal structure.³¹ MOFs provide useful opportunities for investigating such single site catalysis, as the metal centers are connected through aromatic carboxylates.³² In addition, many MOFs have labile ligands such as the solvent molecules that are loosely bound with the metal centers, which can be removed to create coordinatively unsaturated active catalytic center. The observed catalytic activity, then, can be related to the availability of desolvated metal centers or clusters.³³ Of the many catalytic

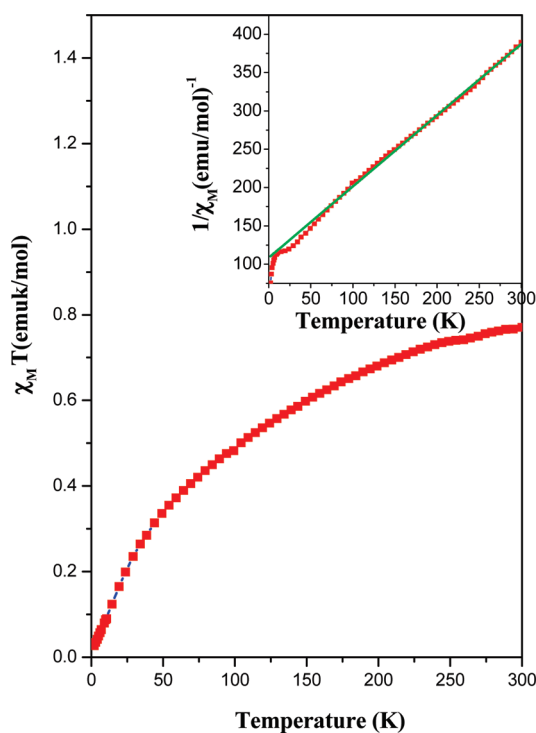
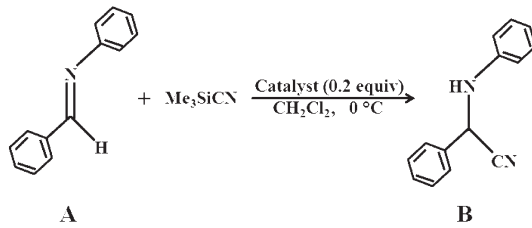


Figure 10. Temperature variation of the $\chi_M T$ for III. The inset shows the corresponding $1/\chi_M$ vs T plots.

reactions, cyanosilylation of imines is used frequently to demonstrate the presence of Lewis acid centers in MOFs. Fujita and co-workers were one of the earliest researchers to exploit the usefulness of the Lewis acid centers by employing the cyanosilylation of carbonyl compounds.³⁴ During the present study, we have isolated three copper-containing compounds, of which two (II and III) have coordinated water molecules. The coordinated water can be removed easily to produce coordinatively unsaturated copper centers, which can act as the Lewis acid. In a typical experiment, activated powdered catalyst (0.03 g of I, 0.033 mmol) was suspended in freshly distilled CH_2Cl_2 solution (10 mL) of imine (A, 0.09 g, 0.5 mmol). Trimethylsilyl cyanide (0.075 g, 0.75 mmol) was added at 0 °C, and the reaction mixture was stirred for 6 h. Similar catalytic conditions and concentrations of the reactants were employed for compounds II and III.



The product, aminonitrile (B), was isolated and analyzed. The control experiments in the absence of the catalyst (copper nitroisophthalate) compounds have also been carried out to ensure that the reaction proceeds catalytically. To make further comparison, we have also carried out the same catalytic reaction in the presence of $\text{Cu}(\text{CH}_3\text{COO})_2 \cdot \text{H}_2\text{O}$ as the catalyst, which exhibited a conversion of ~5–10% to nitrile. The catalytic studies on compound I also exhibited a poor conversion ~7% only, which is comparable to that of the $\text{Cu}(\text{CH}_3\text{COO})_2 \cdot \text{H}_2\text{O}$. Compound II exhibited the maximum conversion with a near

quantitative formation of the aminonitrile (~95%). Compound III exhibited a conversion of ~53%. The catalytic behavior of the three compounds may be correlated with the structure. As can be noted, in compound I, the copper centers are fully coordinated by the ligands, and the bulky aromatic units probably inhibit the approach of the imine to the metal center (Lewis site) to have any meaningful catalytic behavior. Compounds II and III, on the other hand, have a coordinated water molecule, which are labile and can be removed to provide the necessary Lewis acid center for the catalytic reaction. The higher yield in the case of compound II could be due to the presence of two coordinated water molecules. This would impart higher Lewis acidic character in II. In III, of the two copper centers, only one has a coordinated water molecule, which on dehydration gives rise to the Lewis acid center. It is not surprising that III exhibits a reasonable catalytic activity but less than that of II. The spent catalysts were found to be stable as they exhibited the same XRD pattern as that of the fresh catalyst. This suggests that the nitroisophthalate compounds are stable under the experimental conditions. We have also repeated the cyanosilylation studies on the used catalyst, which indicated that the catalytic conversion of imines was comparable to the studies performed using the fresh catalyst. This study suggests that the copper nitroisophthalate phases can be used as a Lewis acid catalyst in recyclable manner.

CONCLUSIONS

The present study is an attempt to employ HT screening as a possible means of identifying new compounds along with the stability ranges as a function of temperature, time, and composition during the formation of MOFs from a complex multicomponent mixture of chemicals. The studies have given rise to six new compounds in the mixture involving copper salts, aromatic acid, and heterocyclic ligand. Of these, three compounds, $[\text{Cu}_3\{(\text{NO}_2)-\text{C}_6\text{H}_3-(\text{COO})_2\}_3(\text{C}_3\text{N}_6\text{H}_6)]$ (I), $[\text{Cu}_2(\mu_3-\text{OH})(\text{H}_2\text{O})\{(\text{NO}_2)-\text{C}_6\text{H}_3-(\text{COO})_2\}(\text{CN}_4\text{H})] \cdot (\text{H}_2\text{O})$ (II), and $[\text{Cu}_2(\mu_3-\text{OH})(\text{H}_2\text{O})\{(\text{NO}_2)-\text{C}_6\text{H}_3-(\text{COO})_2\}(\text{CN}_5\text{H}_2)] \cdot 2(\text{H}_2\text{O})$ (III) have been successfully synthesized in single crystalline form by the use of conventional hydrothermal approaches. The HT study clearly indicated the stability trends in the formation of three new phases. The compounds $\text{Cu}_2\{(\text{NO}_2)-\text{C}_6\text{H}_3-(\text{COO})_2\}(\text{CN}_4\text{H})(\text{H}_2\text{O})$ (IIa), $\text{Cu}_2\{(\text{NO}_2)-\text{C}_6\text{H}_3-(\text{COO})_2\}\{(\text{CN}_5\text{H}_2)\}$ (IIIa), and $\text{Cu}_2\{(\text{NO}_2)-\text{C}_6\text{H}_3-(\text{COO})_2\}\{(\text{CN}_5\text{H}_2)_2\}2\text{H}_2\text{O}$ (IIIb) have been isolated as microcrystalline products. The structural studies indicate that the connectivity between the copper and the NIPA as well as copper and heterocyclic ligand form identifiable units, which are linked together, forming the final two- (II) and three-dimensional (I and III) structures. The bound and lattice water molecules in II and III could be reversibly removed. The dehydrated phase of III has a comparable structure as the parent hydrated phase, although the single crystalline nature appears to be lost upon dehydration. Magnetic studies indicate a predominant antiferromagnetic behavior with a possible canting of the copper spins. Lewis acid catalytic studies suggest that the dehydrated compounds (II and III) are good catalysts for the cyanosilylation of imines. Further work is required to employ the HT method fruitfully in the identification and isolation of newer compounds.

ASSOCIATED CONTENT

S Supporting Information. Simulated and experimental powder XRD patterns, TGA curves, IR spectra, topological

analysis, EPR spectra, bond angles and magnetic plots of the compounds, cyclic TGA of compound **III**, and the Le Bail fit for compounds **IIa**, **IIIa**, and **IIIb** and dehydrated compound **III**. This material is available free of charge via the Internet at <http://pubs.acs.org>.

■ AUTHOR INFORMATION

Corresponding Author

*E-mail: snatarajan@sscu.iisc.ernet.in.

■ ACKNOWLEDGMENT

S.N. thanks the Department of Science and Technology (DST), Government of India, for the award of a research grant under the DST-DAAD program. The Council of Scientific and Industrial Research (CSIR), Government of India, is thanked for the award of a fellowship (D.S.). S.N. also thanks the Department of Science and Technology, Government of India, for the award of the RAMANNA fellowship.

■ REFERENCES

- (1) (a) Furukawa, H.; Ko, N.; Go, Y. B.; Aratani, N.; Choi, S. B.; Choi, E.; Yazaydin, A. O.; Snurr, R. Q.; O'Keeffe, M.; Kim, J.; Yaghi, O. M. *Science* **2010**, *329*, 424. (b) Zhang, J.; Chen, S.; Nieto, R. A.; Wu, T.; Feng, P.; Bu, X. *Angew. Chem., Int. Ed.* **2010**, *49*, 1. (c) Special Issue on MOF. *Chem. Soc. Rev.* **2009**, *38*, 1213–1504. (d) Mahata, P.; Natarajan, S. *Chem. Soc. Rev.* **2009**, *38*, 2304. (e) Maspoch, D.; Ruiz-Molina, D.; Veciana, J. *Chem. Soc. Rev.* **2007**, *36*, 770.
- (2) (a) Farha, O. K.; Malliakas, C. D.; Kanatzidis, M. G.; Hupp, J. T. *J. Am. Chem. Soc.* **2010**, *132*, 950. (b) Xu, G. C.; Ma, X. M.; Zhang, L.; Wang, Z. M.; Gao, S. *J. Am. Chem. Soc.* **2010**, *132*, 9558. (c) Nguyen, J. G.; Cohen, S. M. *J. Am. Chem. Soc.* **2010**, *132*, 4560. (d) Jiang, D.; Urakawa, A.; Yulikov, M.; Mallat, T.; Jeschke, G.; Baiker, A. *Chem.—Eur. J.* **2009**, *15*, 12255. (e) Zhang, B.; Wang, Z. M.; Fujiwara, H.; Kobayashi, H.; Kurmoo, M.; Inoue, K.; Mori, T.; Gao, S.; Zhang, Y.; Zhu, D. *Adv. Mater.* **2005**, *17*, 1988.
- (3) (a) Alkordi, M. H.; Brant, J. A.; Wojtas, L.; Kravtsov, V. C.; Cairns, A. J.; Eddaoudi, M. *J. Am. Chem. Soc.* **2009**, *131*, 17753. (b) Chun, H.; Jung, H. *Inorg. Chem.* **2009**, *48*, 417. (c) Cairns, A. J.; Perman, J. A.; Wojtas, L.; Kravtsov, V. C.; Alkordi, M. H.; Eddaoudi, M.; Zaworotko, M. *J. Am. Chem. Soc.* **2008**, *130*, 1560. (d) Liu, Y.; Kravtsov, V. C.; Eddaoudi, M. *Angew. Chem., Int. Ed.* **2008**, *47*, 8449. (e) Eddaoudi, M.; Kim, J.; Rosi, N.; Vodak, D.; Wachter, J.; O'Keeffe, M.; Yaghi, O. M. *Science* **2002**, *295*, 469.
- (4) (a) Xu, G. F.; Wang, Q. L.; Gamez, P.; Ma, Y.; Clerac, R.; Tang, J.; Yan, S. P.; Cheng, P.; Liao, D. Z. *Chem. Commun.* **2010**, 1506. (b) Zhu, X.; Zhao, J. W.; Li, B. L.; Song, Y.; Zhang, Y. M.; Zhang, Y. *Inorg. Chem.* **2010**, *49*, 1266. (c) Arai, L.; Nadeem, M. A.; Bhadbhade, M.; Stride, J. A. *Dalton Trans.* **2010**, 3372. (d) Cheng, X.; Zhang, W. X.; Lin, Y. Y.; Zheng, Y. Z.; Chen, X. M. *Adv. Mater.* **2007**, *19*, 1494. (e) Maspoch, D.; Domingo, N.; Roques, N.; Wurst, K.; Tejada, J.; Rovira, C.; Ruiz-Molina, D.; Veciana, J. *Chem.—Eur. J.* **2007**, *13*, 8153. (f) Wang, Z.; Zhang, B.; Kurmoo, M.; Green, M. A.; Fujiwara, H.; Otsuka, T.; Kobayashi, H. *Inorg. Chem.* **2005**, *44*, 1230.
- (5) (a) Mahata, P.; Natarajan, S.; Panissod, P.; Drillon, M. *J. Am. Chem. Soc.* **2009**, *131*, 10140. (b) Mahata, P.; Sen, D.; Natarajan, S. *Chem. Commun.* **2008**, 1278. (c) Kurmoo, M.; Kumagai, H.; Tanaka, M. A.; Inoue, K.; Takagi, S. *Inorg. Chem.* **2006**, *45*, 1627. (d) Anokhina, E. V.; Jacobson, A. J. *J. Am. Chem. Soc.* **2004**, *126*, 3044. (e) Konar, S.; Mukherjee, P. S.; Zangrando, E.; Lloret, F.; Chaudhuri, N. R. *Angew. Chem., Int. Ed.* **2002**, *41*, 1561.
- (6) (a) Luo, F.; Che, Y. X.; Zheng, J. M. *Cryst. Growth Des.* **2009**, *9*, 1066. (b) Xia, C.-K.; Lu, C.-Z.; Yuan, D.-Q.; Zhang, Q.-Z.; Wu, X.-Y.; Xiang, S.-C.; Zhang, J.-J.; Wu, D.-M. *CrystEngComm* **2006**, *8*, 281. (c) Lu, T.-B.; Xiang, H.; Luck, R. L.; Mao, Z.-W.; Chen, X.-M.; Ji, L.-N. *Inorg. Chim. Acta* **2003**, *355*, 229. (d) Kurmoo, M.; Kumagai, H.; Green, M. A.; Lovett, B. W.; Blundell, S. J.; Ardavan, A.; Singleton, J. *J. Solid State Chem.* **2001**, *159*, 343. (e) Huang, Z.-L.; Drillon, M.; Masciocchi, N.; Sironi, A.; Zhao, J.-T.; Rabu, P.; Panissod, P. *Chem. Mater.* **2000**, *12*, 2805.
- (7) Chui, S. S. Y.; Lo, S. M. F.; Charmant, J. P. H.; Orpen, A. G.; Williams, I. D. *Science* **1999**, *283*, 1148.
- (8) (a) Murray, L. J.; Dinca, M.; Yano, J.; Chavan, S.; Bordiga, S.; Brown, C. M.; Long, J. R. *J. Am. Chem. Soc.* **2010**, *132*, 7856. (b) Zhang, Z. L.; Shen, G. L.; Cheng, Y.; Ding, Y. B.; Yin, Y. G.; Li, D. *CrystEngComm* **2010**, *12*, 1171. (c) Guo, X.; Zhu, G.; Li, Z.; Chen, Y.; Li, X.; Qiu, S. *Inorg. Chem.* **2007**, *46*, 4065. (d) Pascu, M.; Lloret, F.; Avarvari, N.; Julve, M.; Andruh, M. *Inorg. Chem.* **2004**, *43*, 5189. (e) Ferey, G.; Serre, C.; Millange, F.; Mellot-Draznieks, C.; Surble, S.; Dutour, J.; Margioliaki, I. *Angew. Chem., Int. Ed.* **2004**, *43*, 6269. (f) Ferey, G.; Mellot-Draznieks, C.; Serre, C.; Millange, F.; Dutour, J.; Surble, S.; Margioliaki, I. *Science* **2005**, *309*, 2040. (g) Kim, J.; Chen, B.; Reineke, T. M.; Li, H.; Eddaoudi, M.; Moler, D. B.; O'Keeffe, M.; Yaghi, O. M. *J. Am. Chem. Soc.* **2001**, *123*, 8239. (h) Gutschke, S. O. H.; Molinier, M.; Powell, A. K.; Winpenny, R. E. P.; Wood, P. T. *Chem. Commun.* **1996**, 823.
- (9) (a) Yang, E. C.; Liu, Z. Y.; Shi, X. J.; Liang, Q. Q.; Zhao, X. J. *Inorg. Chem.* **2010**, *49*, 7969. (b) Mahata, P.; Natarajan, S. *CrystEngComm* **2009**, *11*, 560. (c) Mahata, P.; Raghunathan, R.; Banerjee, D.; Sen, D.; Ramasesha, S.; Bhat, S. V.; Natarajan, S. *Chem. Asian J.* **2009**, *4*, 936. (d) Novitchi, G.; Wernsdorfer, W.; Chibotaru, L. F.; Costes, J. P.; Anson, C. E.; Powell, A. K. *Angew. Chem., Int. Ed.* **2009**, *48*, 1614. (e) Li, Z.; Zhu, G.; Guo, X.; Zhao, X.; Jin, Z.; Qiu, S. *Inorg. Chem.* **2007**, *46*, 5174. (f) Xie, L.; Liu, S.; Gao, C.; Cao, R.; Cao, J.; Sun, C.; Su, Z. *Inorg. Chem.* **2007**, *46*, 7782.
- (10) (a) Ren, H.; Song, T. Y.; Xu, J. N.; Jing, S. B.; Yu, Y.; Zhang, P.; Zhang, L. R. *Cryst. Growth Des.* **2009**, *9*, 105. (b) Du, M.; Zhang, Z. H.; You, Y. P.; Zhao, X. J. *CrystEngComm* **2008**, *10*, 306. (c) Ye, J.; Zhang, J.; Ye, L.; Xie, D.; Xu, T.; Li, G.; Ning, G. *Dalton Trans.* **2008**, 5342. (d) Ye, J.; Zhang, J.; Ning, G.; Tian, G.; Chen, Y.; Wang, Y. *Cryst. Growth Des.* **2008**, *8*, 3098. (e) Zhang, H. T.; Li, Y. Z.; Wang, H. Q.; Nfora, E. N.; You, X. Z. *CrystEngComm* **2005**, *7*, 578.
- (11) (a) Banerjee, R.; Phan, A.; Wang, B.; Knobler, C.; Furukawa, H.; O'Keeffe, M.; Yaghi, O. M. *Science* **2008**, *319*, 939. (b) Stock, N.; Bein, T. *Angew. Chem., Int. Ed.* **2004**, *43*, 749. (c) Stock, N.; Bein, T. *Solid State Sci.* **2003**, *5*, 1207. (d) Choi, K.; Gardner, D.; Hilbrandt, N.; Bein, T. *Angew. Chem., Int. Ed.* **1999**, *38*, 2891. (e) Klein, J.; Lehmann, C. W.; Schmidt, H.-W.; Maier, W. F. *Angew. Chem., Int. Ed.* **1998**, *37*, 3369.
- (12) (a) Morris, W.; Leung, B.; Furukawa, H.; Yaghi, O. K.; He, N.; Hayashi, H.; Houndouougbo, Y.; Asta, M.; Laird, B. B.; Yaghi, O. M. *J. Am. Chem. Soc.* **2010**, *132*, 11006. (b) Park, K. S.; Ni, Z.; Cote, A. P.; Choi, J. Y.; Huang, R.; Uribe-Romo, F. J.; Chae, H. K.; O'Keeffe, M.; Yaghi, O. M. *Proc. Natl. Acad. Sci. U.S.A.* **2006**, *103*, 10186. (c) Banerjee, R.; Furukawa, H.; Britt, D.; Knobler, C.; O'Keeffe, M.; Yaghi, O. M. *J. Am. Chem. Soc.* **2009**, *131*, 3875. (d) Liu, Y.; Kravtsov, V. C.; Larsen, R.; Eddaoudi, M. *Chem. Commun.* **2006**, 1488. (e) Huang, X.-C.; Lin, Y.-Y.; Zhang, J.-P.; Chen, X. M. *Angew. Chem., Int. Ed.* **2006**, *45*, 1557.
- (13) SMART (V 5.628), SAINT (V 6.45a), XPREP, SHELXTL; Bruker AXS Inc.: Madison, WI, 2004.
- (14) Sheldrick, G. M. *Siemens Area Correction Absorption Correction Program*; University of Göttingen: Göttingen, Germany, 1994.
- (15) Sheldrick, G. M. *SHELXL-97 Program for Crystal Structure Solution and Refinement*; University of Göttingen: Göttingen, Germany, 1997.
- (16) Farrugia, J. L. WinGX suite for small-molecule single crystal crystallography. *J. Appl. Crystallogr.* **1999**, *32*, 837.
- (17) (a) Brown, I. D. *Chem. Rev.* **2009**, *109*, 6858. (b) Brown, I. D.; Altermatt, D. *Acta Crystallogr.* **1985**, *B41*, 244.
- (18) Le Bail, A.; Duroy, H.; Fourquet, J. L. *Mater. Res. Bull.* **1988**, *23*, 447–452.
- (19) (a) Yan, Y.; Telepeni, I.; Yang, S.; Lin, X.; Kockelmann, W.; Dailly, A.; Blake, A. J.; Lewis, W.; Walker, G. S.; Allan, D. R.; Barnett, S. A.; Champness, N. R.; Schroder, M. *J. Am. Chem. Soc.* **2010**, *132*, 4092.

- (b) Sun, D.; Ma, S.; Simmons, J. M.; Li, J. R.; Yuan, D.; Zhou, H. C. *Chem. Commun.* **2010**, 1329. (c) Furukawa, H.; Kim, J.; Ockwig, N. W.; O'Keeffe, M.; Yaghi, O. M. *J. Am. Chem. Soc.* **2008**, 130, 11650.
- (20) (a) Desiraju, G. R. *Angew. Chem., Int. Ed. Engl.* **1995**, 34, 2311. (b) Desiraju, G. R. *Perspective in Supramolecular Chemistry: The Crystal as a Supramolecular Entity*; Wiley: Chichester, 1996; p 2.
- (21) (a) Yang, W.; Greenaway, A.; Lin, X.; Matsuda, R.; Blake, A. J.; Wilson, C.; Lewis, W.; Hubberstey, P.; Kitagawa, S.; Champness, N. R.; Schroder, M. *J. Am. Chem. Soc.* **2010**, 132, 14457. (b) Jiao, D.; Biedermann, F.; Tian, F.; Scherman, O. A. *J. Am. Chem. Soc.* **2010**, 132, 15734. (c) Lee, S.-L.; Lin, N.-T.; Liao, W.-C.; Chen, C.-h.; Yang, H.-C.; Luh, T.-Y. *Chem.—Eur. J.* **2009**, 15, 11594. (d) Upadhyay, S.; Ramanan, A. *Cryst. Growth Des.* **2006**, 6, 2066. (e) Hunter, C. A.; Sander, J. K. M. *J. Am. Chem. Soc.* **1990**, 112, 5525. (f) Hunter, C. A.; Singh, J.; Sander, J. K. M. *J. Mol. Biol.* **1991**, 218, 837.
- (22) Frisch, M. J.; Trucks, G. W.; Schlegel, H. B.; Scuseria, G. E.; Robb, M. A.; Cheeseman, J. R.; Montgomery, J. A., Jr.; Vreven, T.; Kudin, K. N.; Burant, J. C.; Millam, J. M.; Iyengar, S. S.; Tomasi, J.; Barone, V.; Mennucci, B.; Cossi, M.; Scalmani, G.; Rega, N.; Petersson, G. A.; Nakatsuji, H.; Hada, M.; Ehara, M.; Toyota, K.; Fukuda, R.; Hasegawa, J.; Ishida, M.; Nakajima, T.; Honda, Y.; Kitao, O.; Nakai, H.; Klene, M.; Li, X.; Knox, J. E.; Hratchian, H. P.; Cross, J. B.; Bakken, V.; Adamo, C.; Jaramillo, J.; Gomperts, R.; Stratmann, R. E.; Yazev, O.; Austin, A. J.; Cammi, R.; Pomelli, C.; Ochterski, J. W.; Ayala, P. Y.; Morokuma, K.; Voth, G. A.; Salvador, P.; Dannenberg, J. J.; Zakrzewski, V. G.; Dapprich, S.; Daniels, A. D.; Strain, M. C.; Farkas, O.; Malick, D. K.; Rabuck, A. D.; Raghavachari, K.; Foresman, J. B.; Ortiz, J. V.; Cui, Q.; Baboul, A. G.; Clifford, S.; Cioslowski, J.; Stefanov, B. B.; Liu, G.; Liashenko, A.; Piskorz, P.; Komaromi, I.; Martin, R. L.; Fox, D. J.; Keith, T.; Al-Laham, M. A.; Peng, C. Y.; Nanayakkara, A.; Challacombe, M.; Gill, P. M. W.; Johnson, B.; Chen, W.; Wong, M. W.; Gonzalez, C.; Pople, J. A. *Gaussian 03*, revision B.05; Gaussian, Inc.: Wallingford, CT, 2003.
- (23) (a) Lama, P.; Aijaz, A.; Sanudo, E. C.; Bharadwaj, P. K. *Cryst. Growth Des.* **2010**, 10, 283. (b) Banerjee, A.; Mahata, P.; Natarajan, S. *Eur. J. Inorg. Chem.* **2008**, 3501. (c) Mahata, P.; Natarajan, S. *Inorg. Chem.* **2007**, 46, 1250. (d) Mahata, P.; Ramya, K. V.; Natarajan, S. *Dalton Trans.* **2007**, 4017.
- (24) (a) Nicola, C. D.; Garau, F.; Gazzano, M.; Monari, M.; Pandolfo, L.; Pettinari, C.; Pettinari, R. *Cryst. Growth Des.* **2010**, 10, 3120. (b) Das, S.; Banerjee, P.; Peng, S.-M.; Lee, G.-H.; Kim, J.; Goswami, S. *Inorg. Chem.* **2006**, 45, 562.
- (25) (a) Sarma, D.; Ramanujachary, K. V.; Lofland, S. E.; Magdaleno, T.; Natarajan, S. *Inorg. Chem.* **2009**, 48, 11660. (b) Luo, F.; Che, Y. X.; Zheng, J. M. *Cryst. Growth Des.* **2009**, 9, 1066.
- (26) Nakamoto, K. *Infrared and Raman Spectra of Inorganic and Coordination Compounds*; Wiley-Interscience Publication: New York, 1963.
- (27) (a) Dick, A.; Rahemi, H.; Krausz, E. R.; Hanson, G. R.; Riley, M. J. *J. Chem. Phys.* **2008**, 129, 214505. (b) Lever, A. B. P. *Inorganic Electronic Spectroscopy*; Elsevier: New York, 1968.
- (28) (a) Demadis, K. D.; Papadaki, M.; Aranda, M. A. G.; Cabeza, A.; Olivera-Pastor, P.; Sanakis, Y. *Cryst. Growth Des.* **2010**, 10, 357. (b) Tran, D. T.; Fan, X.; Brennan, D. P.; Zavalij, P. Y.; Oliver, S. R. J. *Inorg. Chem.* **2005**, 44, 6192.
- (29) (a) Ma, L. F.; Wang, L. Y.; Lu, D. H.; Batten, S. R.; Wang, J. G. *Cryst. Growth Des.* **2009**, 9, 1741. (b) Li, X.-J.; Wang, X. Y.; Gao, S.; Cao, R. *Inorg. Chem.* **2006**, 45, 1508.
- (30) (a) Ji, B.-M.; Deng, D.-S.; Lan, H.-H.; Du, C.-X.; Pan, S.-L.; Liu, B. *Cryst. Growth Des.* **2010**, 10, 2851. (b) Zhang, B.; Zhu, D.; Zhang, Y. *Chem.—Eur. J.* **2010**, 16, 9994. (c) Han, Z. B.; Zhang, G. X.; Zeng, M. H.; Yuan, D. Q.; Fang, Q. R.; Li, J. R.; Ribas, J.; Zhou, H. C. *Inorg. Chem.* **2010**, 49, 769.
- (31) (a) Corma, A. *Chem. Rev.* **1995**, 95, 559. (b) Corma, A. *Chem. Rev.* **1997**, 97, 2373.
- (32) (a) Garibay, S. J.; Wang, Z.; Cohen, S. M. *Inorg. Chem.* **2010**, 49, 8086. (b) Liu, H.; Liu, Y.; Li, Y.; Tang, Z.; Jiang, H. *J. Phys. Chem. C* **2010**, 114, 13362. (c) Phan, N. T. S.; Le, K. A.; Phan, T. D. *Appl. Catal., A* **2010**, 382, 246. (d) Chen, B.; Xiang, S.; Qian, G. *Acc. Chem. Res.* **2010**, 43, 1115. (e) Fei, H.; Rogow, D. L.; Oliver, S. R. J. *J. Am. Chem. Soc.* **2010**, 132, 7202.
- (33) Corma, A.; Garcia, H.; Llabres i Xamena, F. X. *Chem. Rev.* **2010**, 110, 4606.
- (34) Fujita, M.; Kwon, Y. J.; Washizu, S.; Ogura, K. *J. Am. Chem. Soc.* **1994**, 116, 1151.